

# **An all-in-one homogeneous DNA walking nanomachine and its application for intracellular analysis of miRNA**

Muren Hu<sup>1</sup>, Dongsheng Mao<sup>2</sup>, Xiaohao Liu<sup>2</sup>, Lingjie Ren<sup>2</sup>, Mengru Zhou<sup>2</sup>, Xiaoxia Chen<sup>2,3,\*</sup>, and Xiaoli Zhu<sup>2,\*</sup>

<sup>1</sup>Department of General Surgery, Tongji Hospital, Tongji University School of Medicine, Shanghai 200065, P. R. China

<sup>2</sup>Center for Molecular Recognition and Biosensing, School of Life Sciences, Shanghai University, Shanghai 200444, P. R. China

<sup>3</sup>State Key Laboratory of Oncogenes and Related Genes, Shanghai Cancer Institute, Ren Ji Hospital, School of Medicine, Shanghai Jiao Tong University, Shanghai 200032, P. R. China

\*Corresponding authors: [accalia@sjtu.edu.cn](mailto:accalia@sjtu.edu.cn); [xiaolizhu@shu.edu.cn](mailto:xiaolizhu@shu.edu.cn)

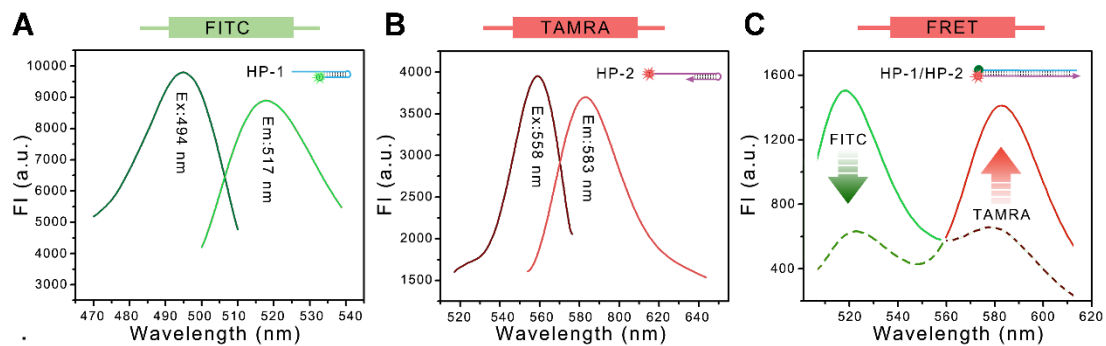


**Figure S1** FRET induced by the hybridization of HP-1 (green) and HP-2 (red). (A) Fluorescence excitation and emission spectra of FITC. (B) Fluorescence excitation and emission spectra of TAMRA. (C) The occurrence of FRET of HP-1/HP-2 after annealing.

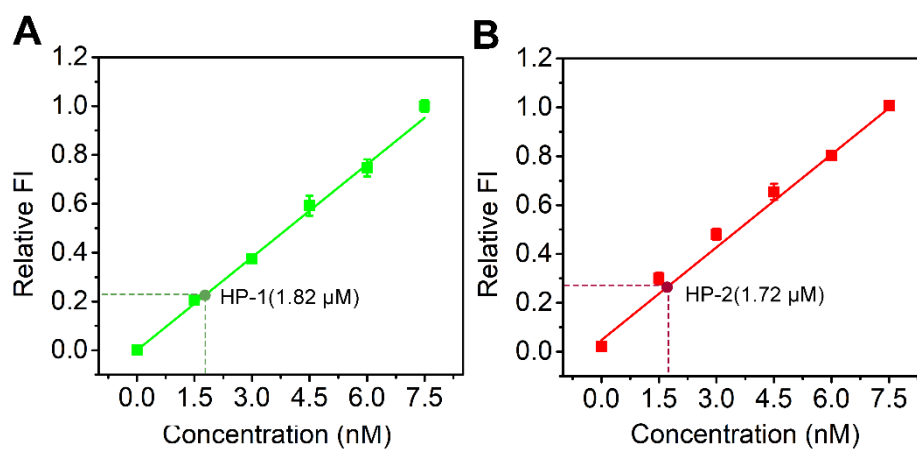


**Figure S2** Standard linear calibration curves of (A) FITC-labeled HP-1 (Ex: 494 nm; Em: 517 nm) and (B) TAMRA-labeled HP-2 (Ex: 558 nm; Em: 583 nm). The intersection points of the dashed lines show the relative fluorescence intensities of HP-1 and HP-2 released from the AuNPs using DTT (10 mM) treatment.

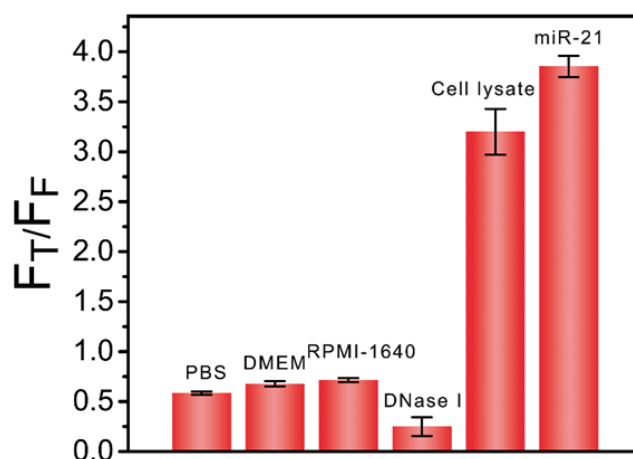


**Figure S3** Fluorescence intensity ratio ( $F_T/F_F$ ) of the nanomachine in the presence of PBS, DMEM with 10% FBS, RPMI-1640 with 10% FBS, DNase I, cell lysate and miR-21.

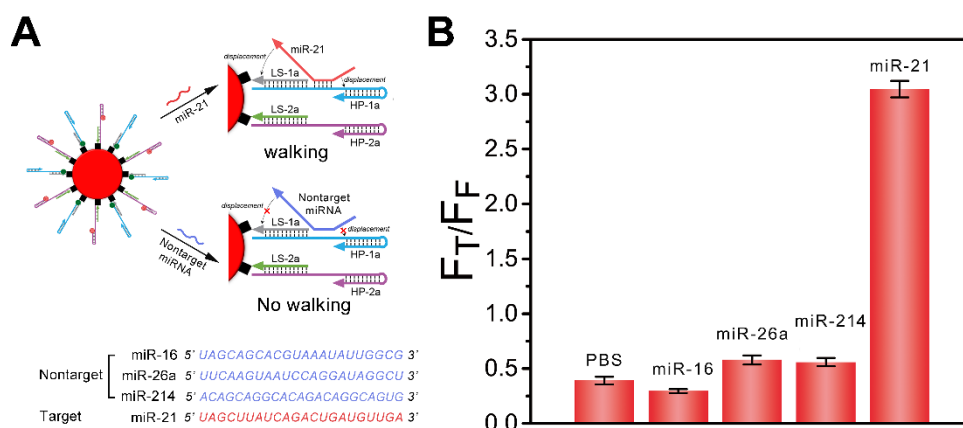


**Figure S4** (A) Scheme showing the nanomachine treated by target miR-21 or nontarget miRNAs (miR-16, miR-26a, and miR-214). (B) Fluorescence intensity ratio ( $F_T/F_F$ ) of the nanomachine in the presence of PBS, miR-16, miR-26a, miR-214, and miR-21.

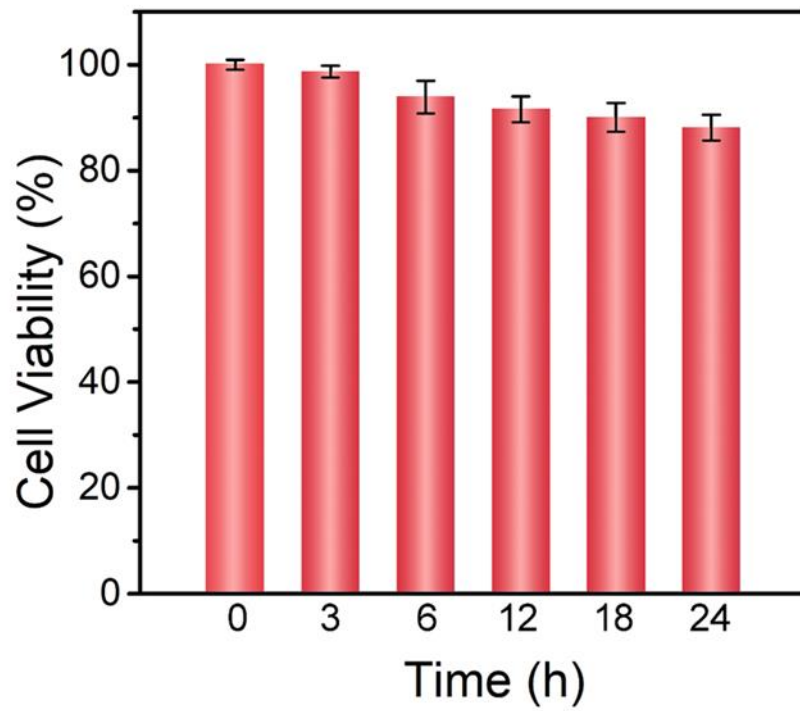


**Figure S5** Cell viability determined by MTT cytotoxicity assays. MCF-7 cells were incubated with nanomachine (6 nM) for 0, 3, 6, 12, 18 and 24 h.

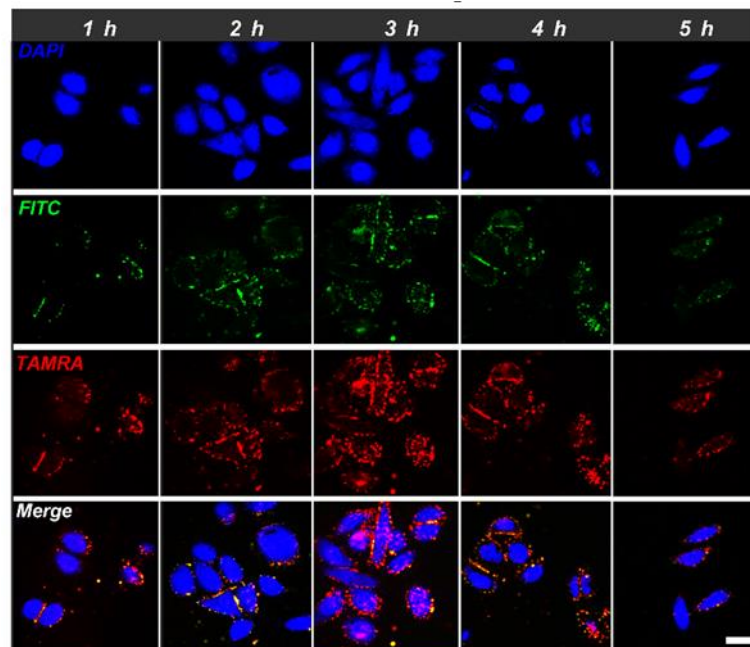


**Figure S6** Confocal images of MCF-7 cells incubated with the nanomachine (6 nM) at different time points. Scale bar: 20  $\mu$ m.

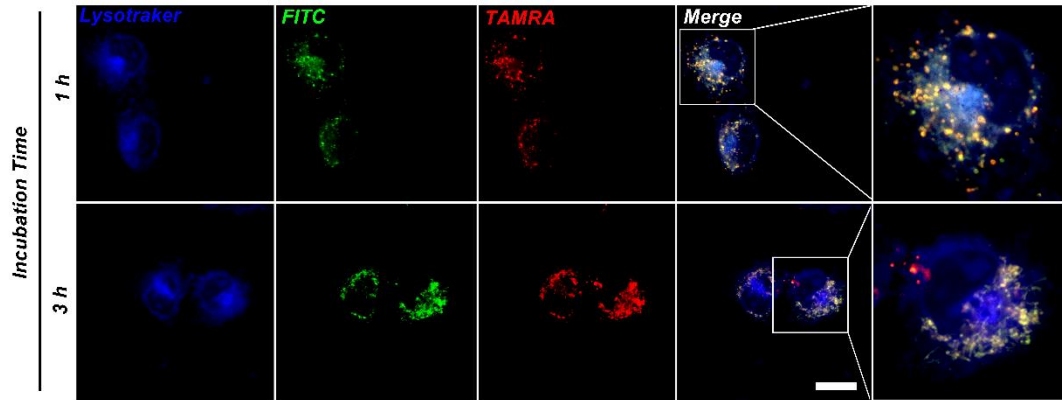


**Figure S7** Confocal images of MCF-7 cells treated with LysoTracker blue and nanomachine for 1 h and 3 h, respectively. Scale bar: 20  $\mu$ m.

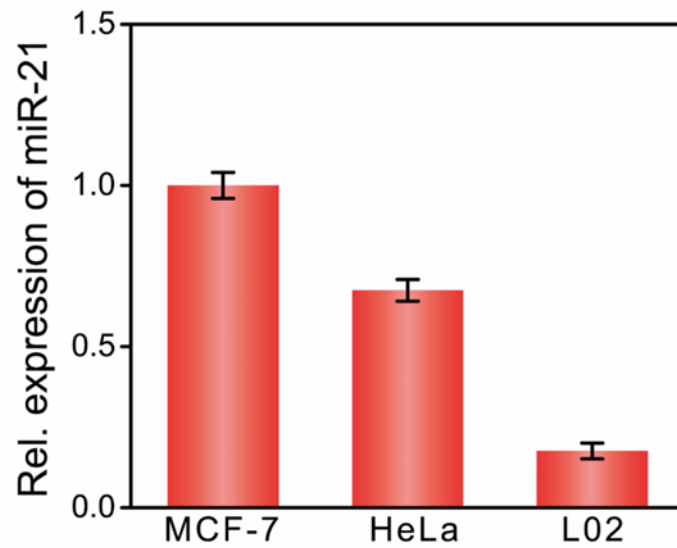


**Figure S8** The relative expression levels of miR-21 in MCF-7, HeLa and L02 by qRT-PCR.

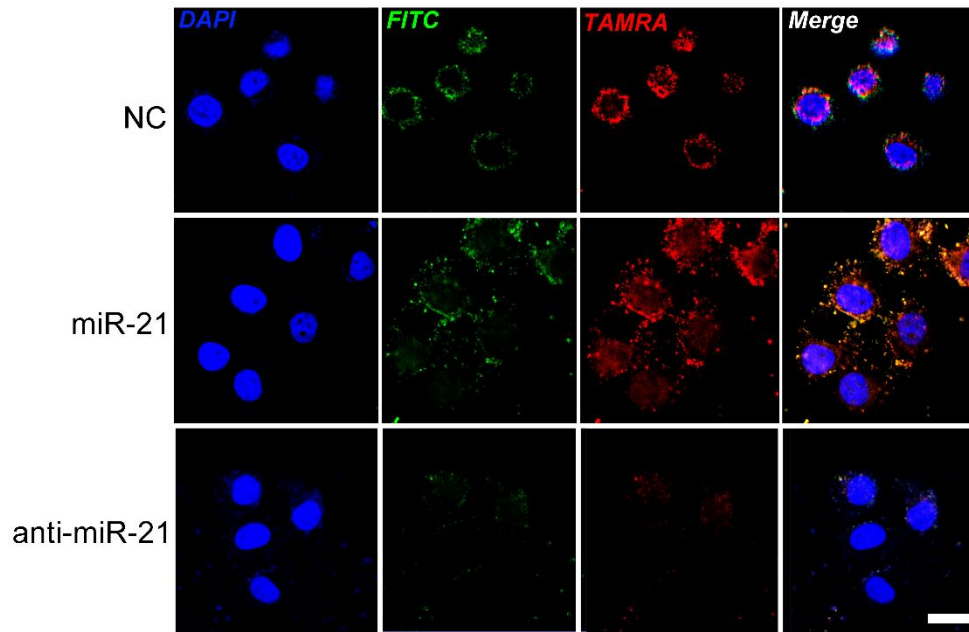


**Figure S9** Confocal images of miR-21 in HeLa cells using the DNA walking nanomachine after transfecting the cells with NC (negative control), miR-21 mimic or inhibitor. Scale bar: 20  $\mu$ m.

**Table S1.** Sequences of oligonucleotides.

Name	Sequence (5' to 3')
LS-1(4 nt)	CAGACTGATGTTGATTT-SH
LS-1(6 nt)	AGACTGATGTTGATTT-SH
LS-1(8 nt)	GACTGATGTTGATTT-SH
LS-2	CTTTGGGGTAGCTTTTT-SH
HP-1(4 nt)	TCAACATCAGTCTGATAAGCTACCCCTTTGGGGTAGC-FITC
HP-1 (6 nt)	TCAACATCAGTCTGATAAGCTACCCCTTTGGGGTAG-FITC
HP-1 (8 nt)	TCAACATCAGTCTGATAAGCTACCCCTTTGGGGTAG-FITC
HP-2	TAMRA-GCTACCCCAAAGGGGTAGCTTATCAGACTGATAGTCTGATAA
Molecular beacon	FITC-TCAACATCAGTCTGATAAGCTAAAAAAAAAAGATGTTGA-BHQ1
miR-21	UAGCUUAUCAGACUGAUGUUGA
miR-21 mimic	UAGCUUAUCAGACUGAUGUUGA
miR-21 inhibitor	TCAACATCAGTCTGATAAGCTA
miR-21 forward	GTGCAGGGTCCGAGGT
miR-21 reverse	GCCGCTAGCTTATCAGACTGATGT
U6 forward	CTCGCTTCGGCAGCAC
U6 reverse	AACGCTTCACGAATTTGCGT
miR-16	UAGCAGCACGUAAAUAUUGGCG
miR-26a	UUCAAGUAAUCCAGGAUAGGCU
miR-214	ACAGCAGGCACAGACAGGCAGU

**Table S2.** Comparison of the assay performance of the nanomachine with previously reported methods for intracellular miRNA detection.

Method	LOD	Readout	Ref.
1 Au Nanoflare Probe	0.68 nM	Fluorescence	1
2 Isothermal Circular Strand Displacement Polymerization (B-ICSDP)	129.4 pM	Fluorescence	2
3 Hairpin-Fuelled Catalytic Nanobeacons	67 pM	Fluorescence	3
4 Single-Layer Perfluorinated Tungsten Diselenide Nanoplatfom	0.75 nM	Fluorescence	4
5 DNAzyme Amplification Strategy	44 pM	Fluorescence	5
6 HCR System	680 pM	Fluorescence	6
7 DNA Walking Nanomachine	26 pM	Fluorescence	This work

## References

1. Zhai LY, Li MX, Pan WL, Chen Y, Li MM, Pang JX, et al. In Situ Detection of Plasma Exosomal MicroRNA-1246 for Breast Cancer Diagnostics by a Au Nanoflare Probe. *ACS Appl Mater Inter.* 2018; 10(46): 39478-39486.
2. Yang Z, Zhang S, Zhao H, Niu H, Wu ZS, Chang HT. Branched DNA Junction-Enhanced Isothermal Circular Strand Displacement Polymerization for Intracellular Imaging of MicroRNAs. *Anal Chem.* 2018; 90: 13891-13899.
3. Wang J, Huang J, Quan K, Li J, Wu Y, Wei Q, et al. Hairpin-Fuelled Catalytic Nanobeacons for Amplified MicroRNA Imaging in Live Cells. *Chem Commun.* 2018; 54(73): 10336-10339.
4. Song Y, Yan X, Ostermeyer G, Li S, Qu L, Du D, et al. Direct Cytosolic MicroRNA Detection Using Single-Layer Perfluorinated Tungsten Diselenide Nanoplatfom. *Anal Chem.* 2018; 90(17): 10369-10376.
5. Li P, Wei M, Zhang F, Su J, Wei W, Zhang Y, et al. Novel Fluorescence Switch for MicroRNA Imaging in Living Cells. *ACS Appl Mater Inter.* 2018; 10(50): 43405-43410.
6. Yang F, Cheng Y, Cao Y, Dong H, Lu H, Zhang K, et al. Sensitively Distinguishing Intracellular Precursor and Mature MicroRNA Abundance. *Chem Sci.* 2018; 10(6): 1709-1715.